

Observations and Models of H-deficient Planetary Nebulae

J. Patrick Harrington

University of Maryland, College Park, MD 20742, USA

Abstract. The number of planetary nebulae which display strong (or complete) depletion of hydrogen is small. This little group is nevertheless very important for the link it establishes to the other highly-evolved, H-deficient stars, and for the samples it provides of highly processed material. This review will emphasize recent WFPC2 imaging and spectroscopy of A30, A78, IRAS 15154-5258 and IRAS 18333-2357. Imaging shows that the inner morphologies of A30 and A78 are strikingly similar, with a clear axial symmetry. IRAS 15154-5258 is seen to be a younger object, where the H-deficient bubble within the H-rich envelope has not yet excavated such a large cavity. IRAS 18333-2357 seems anomalous, but this may only be due to its interaction with the interstellar medium. One of the common characteristics of the H-deficient PNe is their extremely high dust to gas ratio: they all exhibit an anomalous thermal IR luminosity in comparison to their line emission. Modeling such dust-rich gas presents unique problems, as the heating may be controlled by the poorly-known grain photoelectron yields, rather than the more familiar atomic photoionization.

1. Introduction

While many, perhaps most, planetary nebulae (PNe) show evidence of some enrichment with products of nucleosynthesis (e.g., $C/O > 1$, enhanced N), very few are known to contain material which is greatly depleted in hydrogen. The only members of this class that I know of are Abell 30, Abell 78, IRAS 15154-5258, IRAS 18333-2357, and Abell 58¹. Abell 30 was the first such PN discovered (Jacoby 1979; Hazard et al. 1980; Jacoby & Ford 1983) and it remains the best observed. These objects all have a normal (H-rich) nebula which surrounds the H-poor regions. (The exception is IRAS 18333-2357, but here the H-rich shell would doubtless have been swept away by interaction with the ISM.) We do not yet know the true fraction of PNe which contain H-depleted material, as there are obvious selection effects involved in the discovery of these objects.

¹Boroson and Liebert (1989) suggested that the old PN LMC 26 might be hydrogen-poor. A spectrum obtained by Z. Tsvetanov, however, shows hydrogen lines of normal strength.

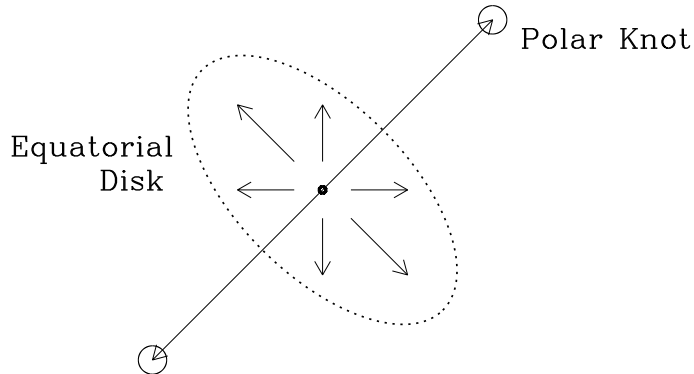


Figure 1. Inner morphology of A30 and A78 (schematic).

2. A30 and A78

2.1. Morphology

The inner regions of A30 and A78 were known to consist of knots of H-poor material, but it was only with the high resolution of the Hubble Space Telescope that the remarkable morphology of these features could be seen. Borkowski, Harrington, Tsvetanov and Clegg (1993) imaged A30 and A78 in the [O III] $\lambda 5007$ line with the HST FOC, and found numerous radial “cometary” structures, produced by the action of the winds from central stars ($\sim 3600 \text{ km s}^{-1}$) sweeping past the H-poor knots. These knots are less than $10''$ from the star and lie within larger wind-blown bubbles with irregular edges which extend to over half the radius of the H-rich envelope. Further imaging by the repaired HST WFPC2 (Borkowski, Harrington and Tsvetanov 1995) showed these features in more detail. Images were also obtained in He I $\lambda 5876$ and He II $\lambda 4686$. These lines are important because the bulk of the knot material is helium, and the surface brightness in these lines provides the density and pressure in the knots. The brightest knot in A30 forms a bow shock facing the star, and it was found that the pressure in this structure is equal to the ram pressure of the stellar wind, which is obtained independently from the wind velocity and mass loss rate. The knot dimensions entail short sound crossing times, implying that they must have cold, neutral cores which are the source of photoevaporative outflows.

The clumps and tails in both objects are arranged in a strikingly similar pattern. In both cases there are a pair of knots which are collinear with the central star, and which thus define an axis. Most of the other knots and their tails appear to be arranged in an equatorial disk perpendicular to this axis. This arrangement is shown schematically in Fig.1; compare with Fig.3 of Borkowski, Harrington and Tsvetanov (1995), the WFPC2 [O III] image.

In A30, the “polar” knots are the brightest of the [O III] features, while in A78 the polar knots are large and diffuse, but are kinematically distinct,

moving outwards at over 100 km s^{-1} (Clegg et al. 1993). In A30 the polar knots differ from the equatorial material both in their spectra and in near IR dust emissivity. The strong axially symmetric morphology of the H-poor knots is in contrast with the surrounding H-rich envelope: A78 has a mildly ellipsoidal shell while the envelope of A30 is quite spherical. Both the spherically symmetric H-rich outer envelope and the axially symmetric H-poor material must have been ejected while the star was a (non-ionizing) asymptotic giant branch star. (The bulk of this material is moving at a few tens of km s^{-1} . Such an ejection velocity implies mass loss from a star with a similar low escape velocity.) Was there a hot, higher-gravity phase between the ejections? How was the stellar envelope spun up to make the second ejection non-spherical? The most plausible mechanism would seem to be tidal interaction with a companion (Livio 1995). Because the polar knots of A30 are precisely collinear with the star – to within $\sim 5'$ – it seems natural to speculate that they may have been formed by the action of a bipolar jet, which would further suggest an accretion disk in a binary system.

We are thus led to what is perhaps the most fundamental question: Can the H-poor PNe be understood as the result of single-star evolution or, conversely, is evolution in an interacting binary system a necessary condition for the formation of H-poor PNe? We recall that it was in fact to explain Abell 30 that Iben, Kaler, Truran and Renzini (1983) devised the (single-star) theory of the rebirth of a PN *via* a late pulse of the helium-burning shell. The evidence is only circumstantial, but the strongly axially symmetric structure of these two nebulae suggests a more complex history, in which binarity of the central star may be crucial for the ejection of the H-poor material.

2.2. The Dust in Abell 30

All the H-poor PNe are extremely dusty, with $L_{IR}/L_{neb} > 10^2$. It was the exceptional IR emission which first called attention to the unusual properties of A30 and A78, while the names of the two *IRAS* objects speak for themselves. The near-IR observations of A30 by Cohen et al. (1977) were puzzling because they found a color temperature of the dust of $\sim 1000 \text{ K}$, while mid-IR measurements indicated a temperature of $\sim 140 \text{ K}$, more typical of PNe. Borkowski et al. (1994) made a detailed study of the IR emission by the dust in A30. They found that the IR spectrum could be well modeled by a power-law distribution of amorphous carbon grains with radii extending down to $\sim 7 \text{ \AA}$. The small grains produce the seemingly high temperatures seen in the near-IR by stochastic heating upon the absorption of single photons, while the larger grains produce the thermal mid-IR emission. The best fit was with a grain size distribution of the form $N(a) \propto a^{-3}$ for $0.0007 \mu\text{m} < a < 0.25 \mu\text{m}$. They also obtained a K-band image which confirmed the earlier findings of Dinerstein and Lester (1984) that the near-IR emission is confined to the equatorial disk and is absent from the polar knots.

By comparison of the *IUE* spectrum of the central star of A30 with a 200,000 K blackbody, Greenstein (1981) recognized that the extinction of this PN was anomalous, and pointed out the similarity of the extinction curve to laboratory measurements of carbon smoke. Jeffery (1995) improved on the analysis by using a model atmosphere to represent the unreddened star. An even simpler approach to the *IUE* data that does not rely on model atmospheres starts

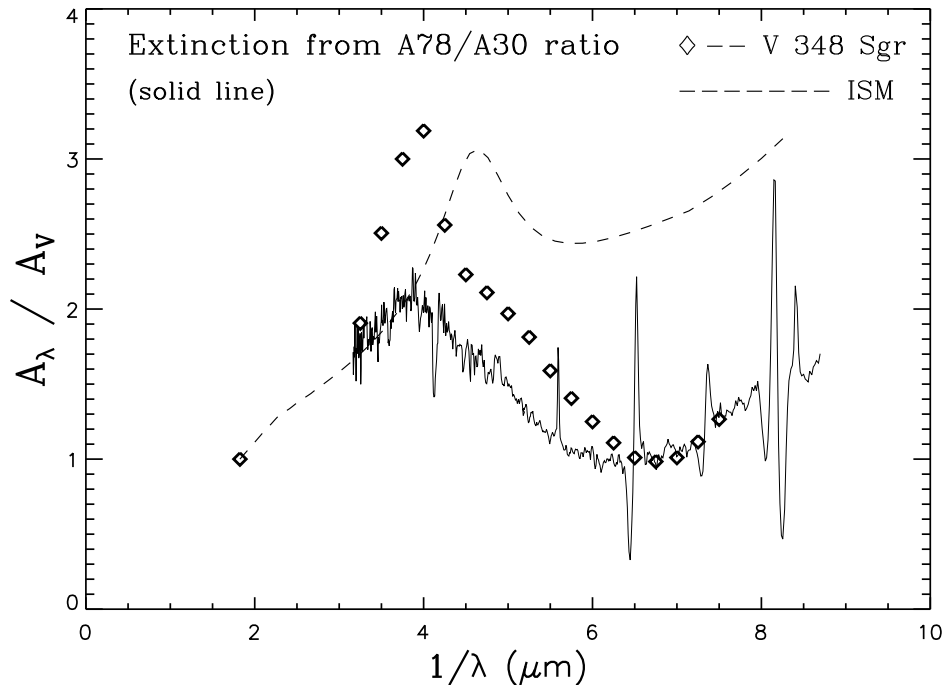


Figure 2. The UV extinction curve of the dust in A30.

with the observation that the central stars of A78 and A30 are very similar. An examination of the WFPC2 images shows that while the central star of A78 is clear of nebulosity, in A30 the clumps of material extend right up to the stellar image. The extinction which A78 does have is most likely that of the ISM; the spectrum has a depression at $\sim 2200\text{\AA}$. We have thus smoothed the spectrum of A78, corrected it for interstellar extinction, and then divided it by the spectrum of A30. The two spectra were normalized at 5480\AA , the effective wavelength of the V filter. The resulting extinction curve for A30, expressed in magnitudes, is plotted in Fig.2. It is quite similar to the result of Jeffery.

It can be seen that the curve is very different from that of the ISM (the P-Cyg profiles should be ignored, as they were smoothed over in the A78 spectrum but not in A30). The extinction has a peak at $\sim 2600\text{\AA}$, as found by both Greenstein and Jeffery. This seems to be a robust result. We also note that the far UV extinction ($\sim 1550\text{\AA}$) is no greater than at V wavelengths. The shape of the curve is very similar the extinction of the dust ejected by V 348 Sgr, the hottest ($T_{eff} = 20,000\text{ K}$) star known to exhibit R CrB-type light variations. V 348 Sgr was observed with *IUE* both before and just after the ejection of a dust cloud, thus permitting “self-calibration” of the attenuated spectrum (Drilling and Schonberner 1989). The extinction peak in V 348 Sgr occurs at the same wavelength as in A30, but is narrower and stronger. This UV extinction curve in combination with the grain-size distribution of Borkowski et al. (1994) should put important constraints on the search for a laboratory analog of the dust. The properties of the amorphous carbon grains discussed by Blanco et al. (1995) look

very promising in this regard, as these particles may exhibit the deep minimum at $\sim 1550\text{\AA}$ seen in Fig.2.

2.3. A Question of Heating

To study the H-poor, dust-rich gas in these nebulae, we should construct **photoionization models**. However, when Harrington and Feibelman (1984) looked at the *IUE* spectra of the knots in A30 they found a major problem: Because of the high abundances of the heavy elements relative to helium, photoionization heating cannot provide sufficient energy input to maintain the observed electron temperature. This can be demonstrated if we compute the ratio of the flux in collisionally excited lines to the flux in a recombination line such as He II $\lambda 1640$. This ratio is a direct measure of the energy input per photoionization; what is known as the “Stoy temperature” of the star. In the knots of A30 the Stoy temperature \gg central star temperature. Harrington and Feibelman concluded that there must be an additional heat source, and suggested heating by electron conduction from the shocked stellar wind². While this is a possibility, such conduction could be strongly inhibited by the presence of even weak magnetic fields. A better solution to the heating problem – a problem which is in fact common to all H-poor PNe – was found by Borkowski and Harrington (1991) in their analysis of IRAS 18333-2357.

3. IRAS 18333-2357: An H-deficient PN in a globular cluster

IRAS 18333-2357 was first detected by the *IRAS* satellite as a strong far-infrared source in the globular cluster M22 (Gillett et al. 1986) and subsequently identified as a peculiar PN (Gillett et al. 1989). It is located about $1'$ from the center of the cluster and is certainly a member on the basis of its radial velocity and proper motion. The nebulosity is $10'' \times 7''$ in size. It is associated with a very hot star, but is quite faint and hard to see in the crowded field. The **only** lines seen are those of [O III] and [Ne III]; no H or He lines have been detected.

IRAS 18333 has a strongly asymmetric, half-moon shaped morphology. This type of asymmetry is the signature of PNe which are interacting with the ISM: the leading side of the object will be compressed, and since the emission from ionized gas is proportional to the square of the density, this type of asymmetry is the result. Borkowski et al. (1993) showed that in the case of IRAS 18333 this morphology results from the motion of M22 through the tenuous ISM ($n_H \sim 0.1 \text{ cm}^{-3}$) with a velocity of 200 km s^{-1} . The nebular material is in fact being stripped from the star and ultimately from the cluster. A corollary is that if IRAS 18333 had an outer envelope of normal (H-rich) composition, it would have already have been stripped away by this process. The interaction with the ISM can give rise to a Rayleigh-Taylor instability, so it is not surprising that the nebula is clumpy: our recent WFPC2 [O III] $\lambda 5007$ images show three main

²Chu and Ho (1995) recently found that A30 is a ROSAT x-ray source, which they claim to be spatially extended. The spectrum corresponds to a $4.5 \times 10^5 \text{ K}$ plasma, cooler than would be expected from the shocked stellar wind, and they discuss the possible importance of conduction in this context.

clumps of emission, two seen earlier with ground-based observations, and a third over the 1"5 distant "companion" to the central star (this star is a background red giant that is not a cluster member).

The central star of IRAS 18333 is of great interest since its cluster membership gives us the distance and some insight into its evolutionary history. Cohen and Gillett (1989) obtained a spectrum which showed He II lines. They confirmed that the star shares the cluster velocity of -153 km s^{-1} and concluded that $T_{eff} \geq 50,000 \text{ K}$. Harrington and Paltoglou (1993) obtained 4m CTIO spectra and detected He II, C IV, N IV and N V lines. Most surprisingly, in view of the absence of hydrogen in the nebula, they found that the wavelength of the He II $\lambda 4338.6 - \text{H}\gamma$ blend showed that H I was the dominant component. The spectrum seems to be close to that of the sdO star KS 292 analyzed by Rauch et al. (1991), which has $T_{eff} = 75,000 \text{ K}$. A temperature this high would imply $L \simeq 14,000 L_{\odot}$, too high for single-star evolution at this epoch in M22. Further analysis of this star, based on HST FOS UV spectra which we have obtained, may provide a more definitive temperature and luminosity.

Gillett et al. (1989) detected only [O III] $\lambda\lambda 5007, 4959$ and [Ne III] $\lambda 3869$ in the nebula. We have obtained ground-based spectra revealing [O III] $\lambda 4363$ from which we find electron temperatures that range from 13,000 K to 20,000 K. No trace of H or He is seen. Any attempt to construct a photoionization model of this nebula flounders on the heating problem. Because no recombination lines of H, He or heavy elements are seen, the gas density must be held low enough to satisfy this constraint. At such low densities, there is not enough heat input to power the observed [O III] $\lambda\lambda 5007, 4959$ lines.

The resolution of this problem lies in the observation that while the luminosity of the nebula in [O III] $\lambda\lambda 5007, 4959$ is only $\sim 0.1 L_{\odot}$, the far-IR luminosity measured by *IRAS* is $\sim 700 L_{\odot}$. This implies a dust/gas ratio $\simeq 0.5$. Under these circumstances, electrons ejected from grains by the photoelectric effect become the major source of heating for the gas. Borkowski and Harrington (1991) constructed photoionization models including heating by photoelectrons from amorphous carbon grains with a power-law size distribution. At each point, it was necessary to solve for the charge of the various grains, as this influences ejected electron spectrum. It was found that such models could explain the observed nebulosity. One facet of this heat source is that, unlike heating by atomic photoionization, it does not scale with gas density or with dilution of radiation in the same way as the cooling; this may lead to large point-to-point temperature variations.

One point to bear in mind is that the yield of photoelectrons is small: for every photon absorbed by a dust grain, less than 1% will result in ejection of an electron. As a result, this process requires a high dust/gas ratio and will always result in a nebula in which $L_{IR} > 100 L_{neb}$.

4. Younger H-poor PNe: IRAS 15154-5258 and Abell 58

Of the H-poor PNe, IRAS 15154, discovered by Manchado et al. (1989), is perhaps the least familiar. It is not far from the galactic plane, and has substantial reddening ($c \sim 1.5$). We have obtained ground-based images and spectra, as well as HST WFPC2 images in $\text{H}\alpha$ and [O III] $\lambda 5007$. This PN has an H-poor core

9" in diameter, where [O III] is very strong, surrounded by an envelope 35" in diameter of normal composition which is best seen in H α . Thus, the H-poor zone is only 1/4 the size of the outer (spherical) shell, unlike A30 and A78, where the H-poor bubble extends over halfway to the edge. While the inner region does not show developed "cometary" features or a distinct axial symmetry, the [O III] image does show radial striations toward the outer part of the core, as well as several radially elongated knots $\sim 0''.9$ from the star. There is no trace of the inner knots in the H α image. In the WFPC2 H α image, we see the outer envelope and a limb-brightened bubble coinciding with the H-poor zone. This bubble is brighter where the [O III] core is brightest, but it does not show the small scale structure seen in the [O III] image. We interpret the H α bubble as the result of H-rich material swept out and compressed by the ejection of the H-poor material. There are two compact structures in the H α image, a radially extended structure $\sim 1''.6$ long located $8''.5$ from the star at p.a. 115° , and a compact but resolved blob $10''.7$ from the star at p.a. 265° . These lie along the direction of features in the [O III] core and indicate some sort of ejection or jet activity. Overall, it looks like IRAS 15154 is at an earlier stage than A30 or A78, so that the ejection of the H-poor material is more recent and only fills a small bubble within the outer nebula. The central star is a WC4 type (Manchado et al. 1989), of lower temperature than A30's $\sim 115,000$ K star. As this nebula evolves, the central star will presumably increase in temperature.

IRAS 15154 has the same heating problem as the other H-poor PNe. From our spectra, we find that $F([\text{O III}])/F(\text{H}\beta) = 74$ in the core; compare this with the ratio of ~ 15 for normal PNe with O^{++} as the major coolant. (The value in the outer shell is 2.) From the [O III] $\lambda 4363/\lambda 5007$ ratio we find $T_e = 20,000$ K in the core. Photoionization by a 50,000 K star can not provide nearly adequate heating. From the *IRAS* far-IR fluxes we find $L_{\text{IR}} = 260 L_\odot$ at an arbitrary distance of 2 kpc. This may be compared to the nebular luminosity. We observe a flux of 3.4×10^{-13} erg cm $^{-2}$ s $^{-1}$ in [O III] $\lambda 5007$. Corrected for reddening, this corresponds to $L_{[\text{O III}]} = 1.2 L_\odot$ at 2 kpc. We would thus require an effective grain photoelectron yield of 0.5% to provide all the energy radiated in the [O III] line. Whether dust heating can provide all the energy radiated by the gas may be an open question, but it surely will be a major energy source for this object.

Finally, a few words about Abell 58. It is the youngest of the H-poor PNe, the ejection of the H-deficient material having been observed as a "nova" around 1919 (V 608 Aql). This material is expanding at several hundred km s $^{-1}$, with the blue-shifted profiles indicating that the optical depth of the dust is high enough to obscure the far side (Seitter 1987, Pollacco et al. 1992). Imaging with HST (Bond et al. 1993) in [O III] $\lambda 5007$ reveals a patchy nebula with a diameter of $0''.5$. Like the other objects, A58 has strong far-IR fluxes.

5. Abundances in H-poor PNe

Because these nebulae provide a bulk sample of material which has undergone H- and He-burning nucleosynthesis, undiluted by envelope material, the exact chemical abundances of the ejecta are of great interest. Unfortunately, several factors make analysis difficult: (1) The nebulosity is faint, so that weaker diagnostic lines are hard to measure. (2) The material is dusty so internal red-

dening may be important, and this dust will have a non-standard extinction curve (see §2.2 above). (3) The material is very inhomogeneous; even at high spatial resolution the spectrum may represent a variety of ionization states and temperatures. In order to extract the most secure information, we would like to construct photoionization models. The exotic composition and the uncertainties in grain photoelectron yields, however, makes this more difficult than for normal PNe. Consequently, the results available at present are somewhat tentative, though some trends are clear.

5.1. A30 and A78

Abundances for A30 and A78 were first obtained by Jacoby and Ford (1983). In A30 they studied two regions, “Knot 3”, our north polar knot, and “Knot 4”, which is the brighter side of the equatorial disk. They found that these regions differed significantly. Relative to He, they obtained for O, N and Ne, respectively: 0.00021, 0.00014 and 0.00007 for the polar knot; 0.0015, 0.00050 and 0.00063 for the equatorial disk; 0.0013, 0.00026 and 0.00055 for A78. In the polar knot (only) they observed a strong C II $\lambda 4267$ recombination line, from which they derived $N(\text{C})/N(\text{He}) = 0.08$, but regarded this result as “uncertain”. Aside from the carbon in the polar knot, they concluded that the other abundances were consistent with a gas of “normal” abundances in which all the H had been converted to He.

Harrington and Feibelman (1984) obtained *IUE* spectra of the region around the north polar knot of A30 by offsetting the large ($10'' \times 20''$) aperture from the central star. They found that C IV $\lambda 1549$ was 9 times stronger than He II $\lambda 1640$, confirming the high C abundance. They concluded that O, N and Ne were also enhanced beyond what would be expected from simple conversion of H to He.

Manchado et al. (1988) analyzed the optical spectrum of A78 in some detail, using a long slit to derive abundances right across the nebula. For the point nearest the star, they obtained abundances, relative to He, of 0.046, 0.046 and 0.0096, for O, N, and Ne, respectively. These values are much higher than those of Jacoby and Ford (1983). While they felt the O and N abundances were uncertain due to the large ionization correction factors needed, neon was observed in three ionization stages and should be secure.

Kingsburgh and Barlow (1994) obtained spectra of the equatorial disk of A30, and found $(\text{O}/\text{He}) \simeq (\text{N}/\text{He}) \simeq (\text{Ne}/\text{He}) \simeq 0.0013$. The O abundance is close to the result of Jacoby and Ford (1983), but the Ne and N abundances are 2-3 times higher; their Ne abundance is to be preferred as they measured the [Ne V] $\lambda 3426$, finding substantial Ne^{+4} . They conclude that beyond conversion of H to He, there is substantial new N and Ne present.

We have recently obtained UV spectra of the H-poor material in A30 using the HST FOS with the $1''$ aperture centered on the north polar knot. A segment of the spectrum is shown in Fig.3 to illustrate the quality of the data. A preliminary list of the strongest lines is given in Table 1.

This small region emphasizes the low-excitation gas around the neutral knot as opposed to the *IUE* spectra of Harrington and Feibelman (1984), which covered a much larger area in the same north polar quadrant. From the ratio of He I $\lambda 5876$ to He II $\lambda 4686$ we see that $N(\text{He}^+)/N(\text{He}^{+2}) \simeq 5$ in the region sampled here. The ratio of C IV $\lambda 1549$ to C III $\lambda 2297$ implies $T_e = 9600$ K, but

Table 1. Fluxes of UV emission lines in the A30 north polar knot

Ion	λ (Å)	Flux [†]
N IV]	λ 1485	0.3
C IV]	λ 1549	0.8
He II]	λ 1640	1.6
C III]	λ 1909	0.76
C III]	λ 2297	0.086
[Ne IV]	λ 2424	1.1
O III]	λ 3133	0.23
He II]	λ 3204	0.12
He II]	λ 4686	0.18*
[O III]	λ 5007	3.2*
He I]	λ 5876	0.11*

[†]FOS, 1'' aperture. Units: 10^{-14} erg cm⁻² s⁻¹.

*From WFPC2 image integrated over 1'' aperture.

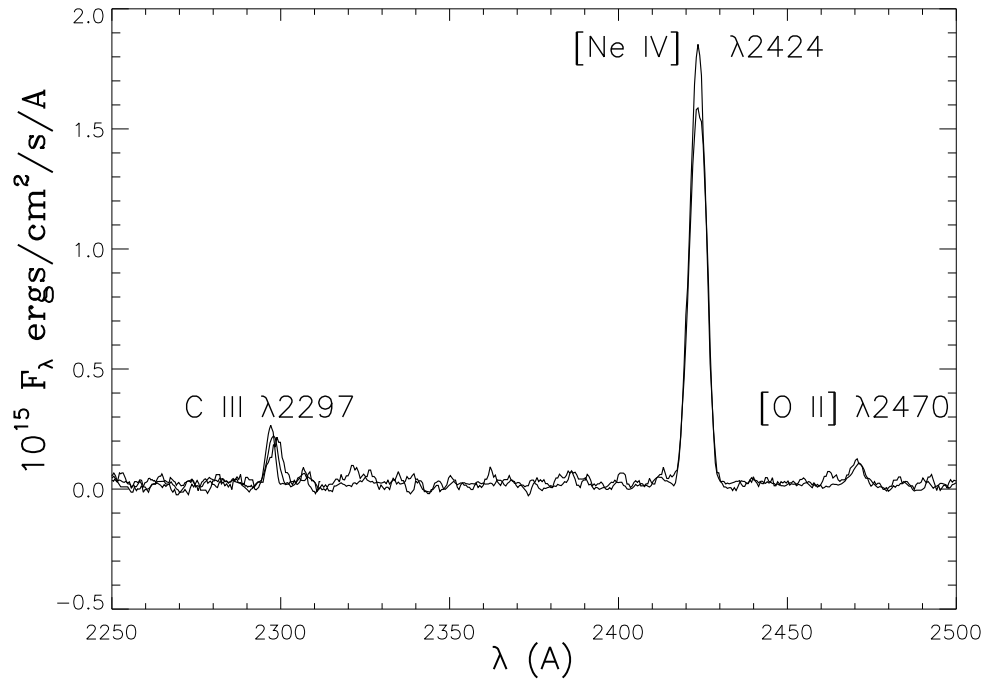


Figure 3. HST FOS spectrum of North Polar Knot of A30. This figure is an overplot of G190H and G270H spectra.

this result neglects extinction and the probable destruction of the C IV resonance line photons by dust. The C^{+3} ions may be found in both the He^+ and He^{+2} zones, which doubtless have very different temperatures; thus even though the temperature dependence of the C III $\lambda 2297$ recombination line is similar to that of He II $\lambda 1640$, the value of $N(C^{+3})/N(He^{+2}) = 0.015$ obtained from this ratio may be misleading. A detailed analysis will be presented elsewhere, but there does appear to be high abundance of C in the polar knot.

The strong [Ne IV] $\lambda 2424$ doublet also implies a high Ne abundance: for an assumed temperature of 15,000 K, we have $N(Ne^{+3})/N(He^{+2}) = 0.0012$. All the Ne^{+3} will be in the He^{+2} zone, but there may be Ne^{+2} and Ne^{+4} there as well, so a lower limit is $N(Ne)/N(He) > 0.0012$.

We note that the O III $\lambda 3133$ line shows that the Bowen fluorescence mechanism is operating in the knot, though comparison with He II $\lambda 3203$ indicates that its efficiency is less than in most PNe.

5.2. IRAS 18333-2357 and IRAS 15154-5258

Borkowski and Harrington (1991) obtained abundances for IRAS 18333-2357 as a by-product of their ionization model of this object. The best model had $(O/He) = 0.015$ and $(Ne/He) = 0.0125$. While the abundances relative to He depend upon the model assumptions – no He lines have been observed – it seems certain that the Ne/O ratio is of the order of unity.

In the case of IRAS 15154-5258, Manchado et al. (1989) found $N(He)/N(H) = 0.40$, $N(O)/N(H) = 0.00115$, $N(Ne^{++})/N(H) = 0.00042$ and $N(N^+)/N(H) = 0.00007$. The H abundance, however, is misleading; our images show that the H lines are projected onto the H-poor core from the surrounding shell (see §4 above) – the core may have little or no H. We find $[Ne\ III] \lambda 3868/[O\ III] \lambda 5007 \simeq 0.24$ after the (uncertain) correction for reddening. Manchado et al. (1989) obtained 0.16 for this ratio; the difference is partly due to their adoption of a smaller reddening.

5.3. Conclusions

The ejecta of the H-poor PNe cannot be explained by merely taking material with typical nebular abundances and converting all the H to He. There are additional enrichments of C, N, perhaps O, and most interestingly, of Ne. If there is at some point substantial N in the He-burning zone of the progenitor star, Ne could be produced by the reactions $^{14}N(\alpha, \gamma)^{18}F(e^+, \nu)^{18}O(\alpha, \gamma)^{22}Ne$.

Acknowledgments. This work was carried out in collaboration with Kazimierz J. Borkowski and Zlatan I. Tsvetanov. Support was provided by NASA through grants G0-3671.01-91A and GO-5404.01-93A from the Space Telescope Science Institute, which is operated by the Association of Universities for Research in Astronomy, Inc., under NASA contract NSA5-26555.

References

- Blanco, A., Fonti, S. and Orofino, V. 1995, ApJ, 448, 339
 Bond, H.E., Meakes, M.G., Liebert, J.W. and Renzini, A. 1993, in IAU Symp. 155, ed. R. Weinberger and A. Acker, (Dordrecht: Kluwer), 499

- Borkowski, K.J. and Harrington, J.P. 1991, *ApJ*, 379, 168
- Borkowski, K.J., Harrington, J.P., Blair, W.P., and Bregman, J.D. 1994, *ApJ*, 435, 722
- Borkowski, K.J., Harrington, J.P., and Tsvetanov, Z. 1993, *ApJ*, 402, L57
- Borkowski, K.J., Harrington, J.P., and Tsvetanov, Z.I. 1995, *ApJ*, 449, L143
- Borkowski, K.J., Harrington, J.P., Tsvetanov, Z.I., and Clegg, R.E.S. 1993, *ApJ*, 415, L47
- Boroson, T.A. and Liebert, J. 1989, *ApJ*, 339, 844
- Chu, Y-H. and Ho, C-H. 1995, *ApJ*, 448, L127
- Clegg, R.E.S., Devaney, M.N., Doel, A.P., Dunlop, C.N., Major, J.V., Myers, R.M. and Sharples, R.M. 1993, in *IAU Symp.* 155, ed. R. Weinberger and A. Acker, (Dordrecht: Kluwer), 388
- Cohen, M. and Barlow, M.J. 1974, *ApJ*, 193, 401
- Cohen, J.C. and Gillett, F.C. 1989, *ApJ*, 346, 803
- Cohen, M., Hudson, H.S., O'Dell, S.L. and Stein, W.A. 1977, *MNRAS*, 181, 233
- Dinerstein, H.L. and Lester, D.F. 1984, *ApJ*, 281, 702
- Drilling, J.S. and Schonberner, D. 1989, *ApJ*, 343, L45
- Gillett, F.C., Jacoby, G.H., Joyce, R.R., Cohen, J.G., Neugebauer, G., Soifer, B.T., Nakajima, T. and Matthews, K. 1989, *ApJ*, 338, 862
- Gillett, F.C., Neugebauer, G., Emerson, J.P. and Rice, W.L. 1986, *ApJ*, 300, 722
- Greenstein, J.L. 1981, *ApJ*, 245, 124
- Harrington, J.P., Borkowski, K.J., and Tsvetanov, Z.I. 1995, *ApJ*, 439, 264
- Harrington, J.P. and Feibelman, W.A. 1984, *ApJ*, 277, 716
- Harrington, J.P. and Paltoglou, G. 1993, *ApJ*, 411, L103
- Hazard, C., Terlevich, B., Morton, D.C., Sargent, W.L.W., and Ferland, G. 1980, *Nature*, 285, 463
- Iben, I., Kaler, J.B., Truran, J.W. and Renzini, A. 1983, *ApJ*, 264, 605
- Jacoby, G.H. 1979, *PASP*, 91, 754
- Jacoby, G.H. and Ford, H.C. 1983, *ApJ*, 266, 298
- Jeffery, C.S. 1995, *A&A*, 299, 135
- Kingsburgh, R.L. and Barlow, M.J. 1994, *MNRAS*, 271, 257
- Livio, M. 1995, in *Asymmetrical Planetary Nebulae*, eds. A. Harpaz and N. Soker (Bristol: Institute of Physics Publishing), p. 51
- Manchado, A., Garcia-Lario, P. and Pottasch, S.R. 1989, *A&A*, 218, 267
- Manchado, A., Pottasch, S.R. and Mampaso, A. 1988, *A&A*, 191, 128
- Pollacco, D.L., Lawson, W.A., Clegg, R.E.S. and Hill, P.W. 1992, *MNRAS*, 257, 33P
- Rauch, T., Heber, U., Werner, K. and Neckel, T. 1991, *A&A*, 241, 457
- Seitter, W.C. 1987, *Messenger*, 50, 14